Indian Journal of Chemistry
Vol. 55A, June 2016, pp. 657-663

# Computational studies on chemically engineered carbon nanotubes as HCl sensor

Taghi Haghtalab[a] & Hamed Soleymanabadi[b,]*

[a]Department of Chemistry, Payame Noor University, 19395-4697, Tehran, Iran

[b]Young Researchers and Elite club, Shahr-e Rey Branch, Islamic Azad University, Tehran, Iran

Email: soleymanabadi.h@gmail.com

*Received 13 September 2015; revised and accepted 16 May 2016*

The effect of functionalization on the sensing properties of a single-walled carbon nanotube in terms of work function and HOMO-LUMO gap changes has been studied by using density functional calculations. Our findings explain the experimental data on the electrical behavior of the SWNTs upon HCl adsorption. Protonation of the basic group induces an electron transfer from the semiconducting SWNTs, thereby altering the HOMO and LUMO levels and significantly changing the electronic properties and work function. The performance of the pyridinol functionalized SWNT as an HCl gas sensor is shown to be superior to the other studied materials, in terms of both response signal and reversibility time. These results are in good agreement with the experimental reports.

**Keywords:** Theoretical chemistry, Electronic properties, Sensors, Hydrogen chloride sensors, Nanostructures, Carbon nanotubes, Functionalised carbon nanotubes

Nanostructure gas sensors work based on the monitoring the direct change in their electrical properties in response to the interaction with gas molecules.[1-7] One-dimensional nanotubes are the ideal molecular wires with highly robust structures, which provide the components necessary for large-scale integration into advanced sensor devices.[8-13] In some cases, the adsorbate molecules do not affect the electronic properties of the nanostructures due to weak interaction.[14-16] It has been shown that creating a defect, functionalization, and doping metals or metal oxide nanoparticles can improve the sensitivity of these materials to gas molecules.[17-22] It has been previously reported that covalent functionalization dramatically increases the change in resistance of single-walled carbon nanotube (SWNT) films during exposure to gas molecules.[23] Facile dispersibility in solvents, reproducible and well-defined chemical composition, and possibility of attaching organic moieties specifically engineered to interact with analyte molecules are the major advantages of the covalently functionalized SWNT materials.

HCl gas is primarily produced by incineration of halogenated polymers, burning of plants, and absorption tower of semiconductor factories.[24] The concentrations of HCl gas are strictly regulated in the workplace because the gas is harmful to the human body.[25] An efficient HCl sensor with high sensitivity and reliability is in demand to monitor the release of HCl into the environment. Bekyarova *et al.*[26] have employed chemically functionalized SWNTs with a range of basicity and electronic structures, and explored the change of their electronic properties on exposure to hydrogen chloride (HCl). Towards this aim, they synthesized three types of functionalized SWNT materials (amide functionalized (SWNT-$CONH_2$, **A**), octadecylamine functionalized (SWNT-$CONH(CH_2)_{17}CH_3$, **B**) and pyridinol functionalized (SWNT-$COOC_5H_4N$, **C**) with covalently attached functional groups of varying basicity and compared the change in their electronic properties with that of purified non-functionalized SWNTs on exposure to HCl. Herein, we have investigated the response of pristine SWNT and functionalized materials toward HCl, based on the density functional theory calculations, and compared the results with the experimental results.

## Computational Methodology

We selected a zigzag (8, 0) SWNT (Fig. 1) in which the end atoms were saturated with hydrogen atoms to reduce the boundary effects. Geometry optimizations, energy calculations, and natural bond orbital analysis (NBO) analysis were performed using B3LYP functional augmented with an empirical dispersion term (B3LYP-D)[27], with 6-31G(d) basis set

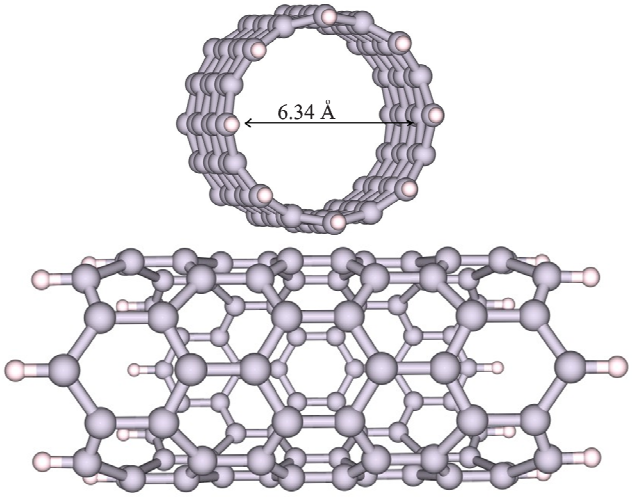


Fig. 1—Optimized structure of zigzag (8,0) single-walled carbon nanotube.

as implemented in GAMESS suite of the program.[28] The B3LYP density functional has been previously shown to reproduce experimental properties and has been commonly used in nanostructure studies.[29-36] It has been also demonstrated that it is reliable in predicting both the ground state energies and the electronic structure.[37,38] We have used the definition of HCl adsorption energy, $E_{ad,}$ as follows:

$$E_{ad} = E\,(\text{HCl/Tube}) - E\,(\text{Tube}) - E\,(\text{HCl}) + E_{BSSE} \ldots (1)$$

where $E$ (HCl/Tube) corresponds to the energy of the pristine or functionalized SWNTs in which the HCl has been adsorbed on the surface, $E$ (Tube) is the energy of the isolated pristine or functionalized SWNTs, $E$ (HCl) is the energy of a single HCl molecule, and $E_{BSSE}$ is the energy of the basis set superposition error. HOMO-LUMO energy gap ($E_g$) is defined as Eq. (2),

$$E_g = E_{LUMO} - E_{HOMO} \quad \ldots (2)$$

where $E_{LUMO}$ and $E_{HOMO}$ are the energy of HOMO and LUMO.

## Results and Discussion

### Geometry parameters and adsorption behavior

The geometry of the optimized SWNT is shown in Fig. 1. The length and diameter of optimized bare CNT were computed to be about 13.56 and 6.34 Å, respectively. First, we investigated the adsorption of an HCl molecule on the surface of the SWNT. Towards this, different initial configurations were tested including the molecule being vertical (from H or Cl atom) or horizontal to the surface of the nanotube. Finally, we predicted only one stable complex in which the HCl molecule is oriented such that its H atom is located on a C atom with interaction distance of 2.49 Å. The molecule is oriented to this position in the other initial structures upon relaxation. The $E_{ad}$ was calculated to be ~ −6.4 kJ/mol and an NBO charge of ~0.041 $e$ transfers from the tube to the molecule. This indicates that the integration is very weak and it may be predicted that the electronic properties of the tube will not change significantly.

### Sensitivity

Here, we used two electronic factors including band gap ($E_g$) and work function ($\Phi$) to probe the sensitivity of the studied adsorbents. It has been frequently shown that a significant change of $E_g$ upon the adsorption process will change the electrical conductivity of the adsorbent by altering the electron population of the conduction band.[39-42] If the sensor material is selected as part of an electronic circuit the sharp change of the conductivity can be inverted to an alarm signal, helping to detect the adsorbate. The modulation of the electronic conductivity of a sensor is a very attractive approach because of its simplicity. It has been shown that the work function is also sensitive to adsorption effects and work function based gas sensors are able to detect chemical species at ambient up to slightly elevated temperatures.[43]

The work function is the least amount of energy required to remove an electron from the Fermi level of a semiconductor to a point far enough not to feel any influence of the substance. The change of work function of an adsorbent after the gas adsorption alters its field emission properties. Work function value was calculated using the following equation:

$$\Phi = E_{inf} - E_F \quad \ldots (3)$$

where $E_{inf}$ is the electrostatic potential at infinity and $E_F$ is the Fermi level energy. Determining the absolute value of a material's work function is very difficult theoretically because the calculation of $E_{inf}$ is not straightforward. However, the absolute value of work function is not our concern and our main focus is on its change ($\Delta\Phi$) upon adsorption process. To this purpose, the electrostatic potential at infinity can be assumed to be zero because this discrepancy does not have a significant impact on the analysis of the relative values of the work function of pure versus complex SWNT, and the aberration can be compensated by the scissors approximation. The work function changes ($\Delta\Phi$) were calculated by subtracting

the work function of the clean nanotube from that of the corresponding adsorbed system. The canonical assumption for Fermi level energy ($E_F$) is that in a molecule (at $T$ = 0 K), it lies approximately in the middle of the $E_g$.[44]

The predicted work function for the SWNT is about 3.67 and 3.72 eV at B3LYP and B3PW91 levels of theory with 6-31G(d) basis set, respectively. It has been previously shown that the work function of SWNTs is in the range 4.95–5.05 eV, based on the photoelectron emission method.[45] Suzuki and co-workers[46] have also shown that the work functions of SWNTs do not seem to have a large structural dependence. It indicates that the DFT levels used significantly underestimate the absolute value of the work function. We found that using Austin Model 1 (AM1)[47] on the optimized structure at B3LYP/ 6-31G(d) (AM1// B3LYP) significantly improves the value of the work function. The calculated work function value for SWNT is ~4.96 eV at AM1// B3LYP level, which is in good agreement with the experimental results.[48] Therefore, we used this strategy to calculate the work function of the all studied systems. As shown in Table 1, the work function of SWNT-HCl is ~4.99 eV, indicating a negligible change (by about 0.60%) upon HCl adsorption. Also, Table 2 shows that the $E_g$ of SWNT is not altered after the HCl adsorption process. These results indicate that the pristine SWNT is not appropriate material for HCl detection. The experimental work shows that the electrical resistance of the pristine tube also exhibits a small change upon exposure to HCl[26]. Such small response of the pristine SWNT may be due to defects and carbonaceous impurities which are not involved here.

Table 1—The work function of the pristine and functionalized SWNT and its change (ΔΦ) after HCl adsorption

| System | Φ(eV) | ΔΦ (eV) | ΔΦ (%) |
|---|---|---|---|
| SWNT | 4.96 | - | - |
| SWNT-HCl | 4.99 | 0.03 | 0.60 |
| **A** | 5.09 | - | - |
| **A**-HCl | 5.27 | 0.18 | 3.53 |
| **B** | 5.07 | - | - |
| **B**-HCl | 5.28 | 0.21 | 4.14 |
| **C** | 5.21 | - | - |
| **C**-HCl | 5.48 | 0.27 | 5.18 |

**Functionalized nanotubes**

We constructed three types of functionalized SWNT materials[26] (**A**, **B**, and **C**) with covalently attached functional groups of varying basicity (Fig. 2) and compared the change of their electronic properties to that of purified non-functionalized SWNT on exposure to HCl. The basicity of the functional groups was in order: $-CONH_2$ > $-CONH(CH_2)_{17}CH_3$ > $-COOC_5H_4N$.[26] It is likely that all of the functionalized SWNTs will undergo protonation due to the strongly acidic character of HCl. This was confirmed by the

Table 2—Calculated energy ($E_{ad}$), HOMO energy ($E_{HOMO}$), LUMO energy ($E_{LUMO}$), and HOMO-LUMO energy gap ($E_g$) of the systems at B3LYP and B3PW91 levels with 6-31G(d)

| | System | $E_{ad}$ (kJ/mol) | Q[a] | $E_{HOMO}$ (eV) | $E_{LUMO}$ (eV) | $E_g$ (eV) | [b]$\Delta E_g$ (%)[b] |
|---|---|---|---|---|---|---|---|
| B3LYP | SWNT | - | - | -3.670 | -3.429 | 0.242 | - |
| | SWNT-HCl | -6.4 | 0.029 | -3.747 | -3.504 | 0.242 | 0.0 |
| | **A** | - | - | -3.775 | -3.533 | 0.241 | - |
| | **A**-HCl | -79.8 | 0.491 | -4.168 | -3.845 | 0.323 | 34.0 |
| | **B** | - | - | -3.746 | -3.505 | 0.241 | - |
| | **B**-HCl | -90.4 | 0.510 | -4.157 | -3.825 | 0.332 | 37.4 |
| | **C** | - | - | -3.990 | -3.758 | 0.231 | - |
| | **C**-HCl | -61.2 | 0.526 | -4.336 | -4.012 | 0.324 | 40.1 |
| B3PW91 | SWNT | - | - | -3.843 | -3.601 | 0.242 | - |
| | SWNT-HCl | -4.1 | 0.035 | -3.915 | -3.673 | 0.242 | 0.0 |
| | **A** | - | - | -3.943 | -3.702 | 0.241 | - |
| | **A**-HCl | -75.5 | 0.509 | -4.338 | -4.022 | 0.316 | 30.9 |
| | **B** | - | - | -3.918 | -3.677 | 0.241 | - |
| | **B**-HCl | -84.8 | 0.531 | -4.322 | -4.001 | 0.321 | 33.1 |
| | **C** | - | - | -4.159 | -3.943 | 0.216 | - |
| | **C**-HCl | -59.3 | 0.582 | -4.503 | -4.212 | 0.291 | 34.7 |

[a]The charge is transferred from the tube to HCl.
[b]The change of HOMO-LUMO gap after HCl adsorption.

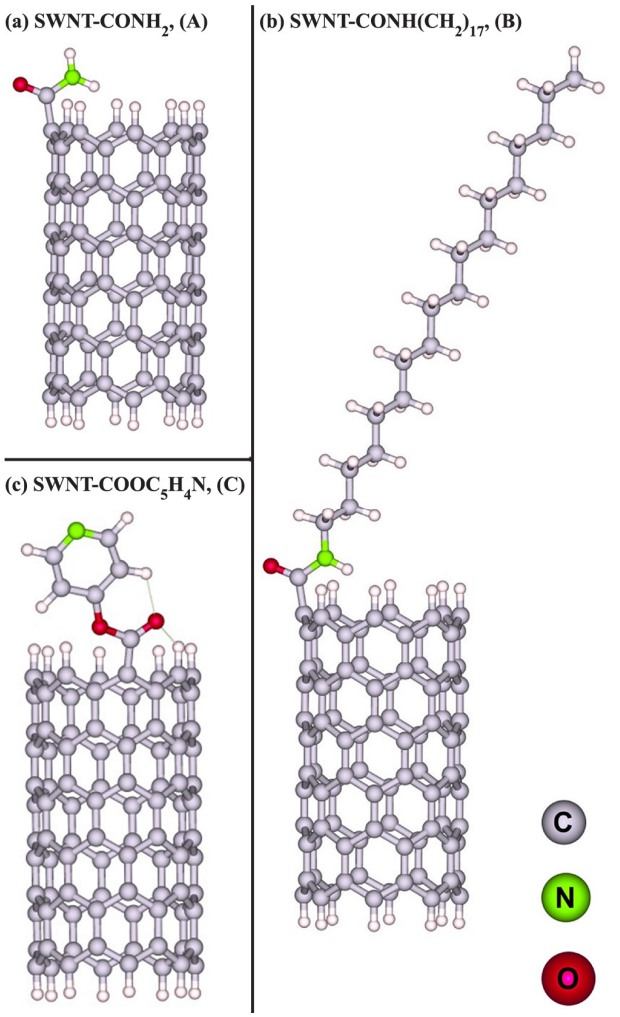


Fig. 2—Optimized structures of (a) the amide functionalized nanotubes (SWNT-$CONH_2$, **A**); (b) octadecylamine functionalized (SWNT-$CONH(CH_2)_{17}CH_3$, **B**) and (c) pyridinol functionalized (SWNT-$COOC_5H_4N$, **C**).

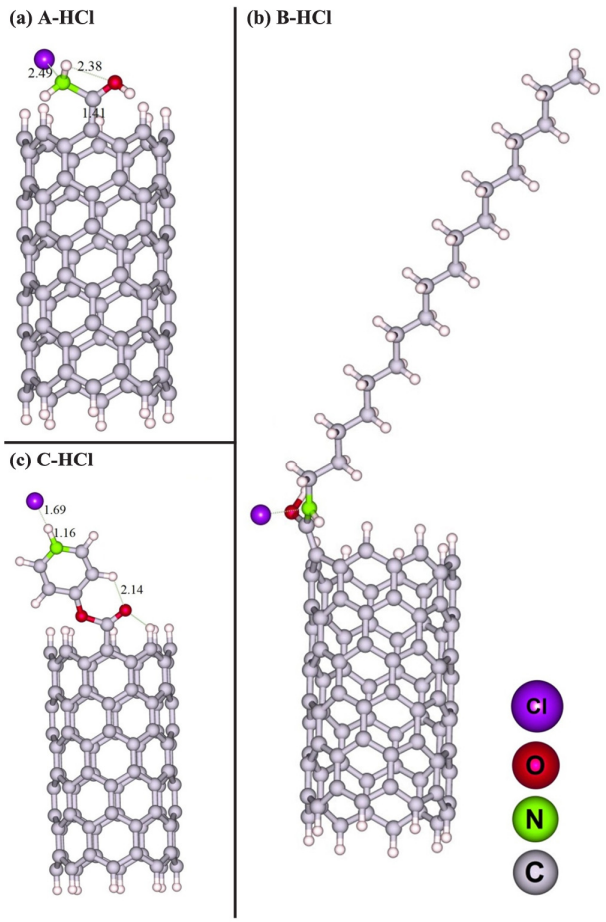


Fig. 3—Optimized structures of the HCl adsorbed functionalized SWCNT systems (a) amide functionalized (SWNT-$CONH_2$, **A**-HCl), (b) octadecylamine functionalized (SWNT-$CONH(CH_2)_{17}CH_3$, **B**-HCl) and (c) pyridinol functionalized (SWNT-$COOC_5H_4N$, **C**-HCl).

experimental work, indicating that the charged conjugate acid is the expected structure of the HCl adsorbed **A**, **B** and **C** complexes. Thus, these complexes were prepared as shown in Fig. 3. In the HCl-**A** and -**B** complexes, the proton H attaches to the oxygen of the tube and the Cl anion is close to the N atom. In the HCl/**C** complex, the N atom of the **C** was protonated.

Table 2 shows that after the HCl adsorption, the LUMO and, particularly, the HOMO of the functionalized SWNTs shift to lower energies and become more stable due to the charge transfer from the tube to the HCl. Subsequently, the $E_g$ was increased by about 34.0%, 37.4% and 40.1% for **A**, **B** and **C**, respectively. The stronger $E_g$ change of the **A**, **B** and **C** films as compared to the pristine SWNT is due to the presence of functional groups, which allow for the direct binding of the HCl molecule, in which the charge redistribution occurred significantly. As the basicity of the functional groups increases, the change of $E_g$ of the SWNT films is increased. The change of work function of the pristine SWNT upon the HCl adsorption is about 0.03 eV (Table 1) which is negligible. After the adsorption process, the work function of **A**, **B** and **C** functionalized tubes is significantly changed by about 0.18, 0.21, and 0.27 eV, respectively. Similar to the $E_g$ change, the change of work function will increase as the basicity of the functional groups increases. Generally, we can conclude that as the basicity of the functional groups increases, the sensitivity of the SWNT films improves.

To further investigate the difference in the interaction of an HCl with the pristine as well as functionalized nanotubes, we have drawn molecular

electrostatic potential surface (MEP) plots for the pristine and sample **C** as a representative functionalized model. The patterns of the MEPs in Fig. 4 show two kinds of interactions: continuous density-rich zone between the H atom of HCl and the N atom of **C** configuration, and the zone which exhibits a clear discontinuity along HCl-tube axes in the complex HCl/tube. The continuous area is typically associated with a strong directional bond creation, which is consistent with the more negative $E_{ad}$ for HCl-C complex. Conversely, discontinuous zone is associated with less directional bonds that are usually weaker which is again consistent with both less negative $E_{ad}$ of HCl/tube.

**Desorption**

Bekyarova *et al.*[26] have illustrated that the performance of the **C** nanotube is superior to that of the other materials in both response signal and reversibility time. About response signal, we have predicted that the electronic properties and work function of the **C** nanotube are more sensitive than those of **A** and **B** toward the HCl adsorption. The reversibility time τ can be given by the conventional transition state theory (Eq. 4),[8]

$$\tau = \upsilon_0^{-1} \exp(- E_{ad}/kT) \quad \ldots (4)$$

where $T$ is the temperature, $k$ is the Boltzmann constant, and $v_0$ is the attempt frequency. Very strong interactions are not favorable in gas detection because these imply that desorption would be difficult and the device may suffer from long recovery times. If the $E_{ad}$ significantly becomes more negative, much longer recovery time is expected based on this equation. More negative $E_{ad}$ values will prolong the recovery time in an exponential manner. However, it is an advantage, the $E_{ad}$ of HCl is not large enough to hinder the recovery of the sensor. The calculated $E_{ad}$ for the HCl adsorption on the **C** is about −61.2 kJ/mol (Table 2) which is less negative than the $E_{ad}$ of HCl/**A** and HCl/**B**. Thus, the recovery time of the **C** film is much shorter than that of the **A** and **B** films which confirms the finding of the experimental work.[26]

**Concentration effects**

We have studied the effect of concentration (or pressure for a gas) on the $E_{ad}$ and electronic properties by increasing the number of adsorbed HCl molecules on the edge of **C** configuration. The second HCl atom tends to attach to the Cl atom of the first HCl as shown in Fig. 5. The calculated $E_{ad}$ per adsorbed HCl is ~ −62.0 kJ/mol, which is not noticeably different from the $E_{ad}$ of one HCl adsorption (–61.2 kJ/mol). The third HCl is also adsorbed similar to the second one on the Cl atom of the first molecule with the $E_{ad}$ ~ –59.7 kJ/mol per molecule. Table 3 indicates that by increasing the number of adsorbed HCl molecules, the change in electronic properties of **C**, especially the $E_g$ is more. Our analysis shows that the second and third HCl molecules cause stronger protonation of N atom of the **C** configuration by increase in weakening of the H-Cl bond of the first HCl. Thus, the charge transfer increases and affects the electronic properties more. The calculated charge transfer is ~0.541 *e* and ~0.559 *e* from **C** to the adsorbed molecules.

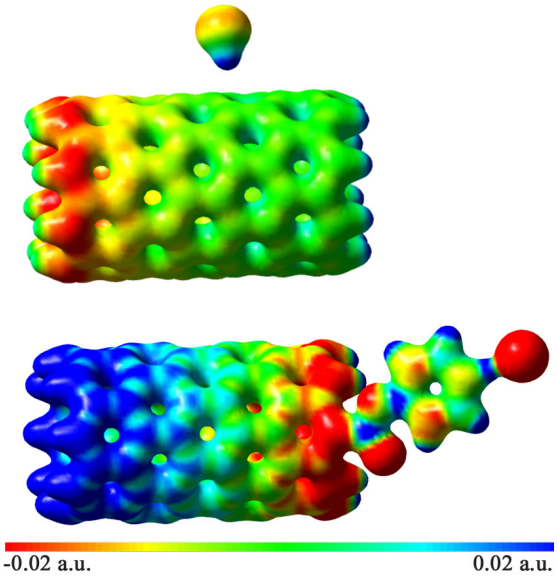


Fig. 4—Molecular electrostatic potential plots for HCl/pristine-tube and HCl-**C** complexes.

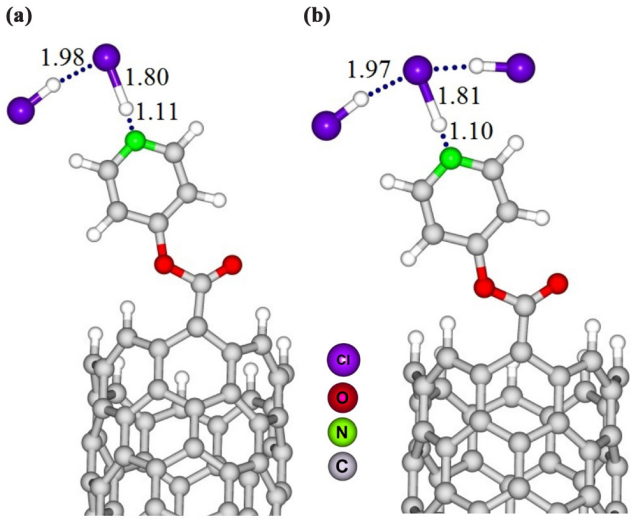


Fig. 5—Optimized structures of two and three HCl molecules adsorbed pyridinol functionalized (SWNT-$COOC_5H_4N$, **C**).

Table 3—Calculated energy per HCl ($E_{ad}$), HOMO energy ($E_{HOMO}$), LUMO energy ($E_{LUMO}$), and HOMO-LUMO energy gap ($E_g$) of the systems at (Fig. 4.) at B3LYP/6-31G(d)

| System | $E_{ad}$ (kJ/mol) | Q[a] | $E_{HOMO}$ (eV) | $E_{LUMO}$ (eV) | $E_g$ (eV) | $\Delta E_g$ (%)[b] |
|---|---|---|---|---|---|---|
| **C** | - | - | -3.990 | -3.758 | 0.231 | - |
| **C**-$(HCl)_2$ | -62.0 | 0.541 | -4.353 | -4.019 | 0.334 | 44.6 |
| **C**-$(HCl)_3$ | -59.7 | 0.559 | -4.359 | -4.021 | 0.338 | 46.3 |

[a]The charge is transferred from the tube to the adsorbate.
[b]The change of HOMO-LUMO gap after HCl adsorption.

Table 4—Calculated energy ($E_{ad}$), HOMO energy ($E_{HOMO}$), LUMO energy ($E_{LUMO}$), and HOMO-LUMO energy gap ($E_g$) of the systems at (Fig. 3.) at different level of theories with 6-31G(d) basis set

| | System | $E_{ad}$ (kJ/mol) | $E_{HOMO}$ (eV) | $E_{LUMO}$ (eV) | $E_g$ (eV) | $\Delta E_g$ (%)[a] |
|---|---|---|---|---|---|---|
| M06-L | **C** | - | -3.890 | -3.991 | 0.101 | - |
| | **C**-HCl | -50.2 | -4.090 | -4.232 | 0.142 | 40.6 |
| M06 | **C** | - | -3.834 | -4.324 | 0.490 | - |
| | **C**-HCl | -61.3 | -4.077 | -4.692 | 0.615 | 25.5 |
| M06-2X | **C** | - | -3.302 | -5.023 | 1.721 | - |
| | **C**-HCl | -67.5 | -3.535 | -5.454 | 1.919 | 11.5 |
| M06-HF | **C** | - | -3.328 | -6.150 | 2.822 | - |
| | **C**-HCl | -71.4 | -3.538 | -6.636 | 3.098 | 9.8 |

[a]The change of HOMO-LUMO gap after HCl adsorption.

**Density functional studies**

For comparison, we optimized all structures and calculated the properties using B3PW91 functional with 6-31G(d) basis set (Table 2). The B3PW91 results for the absolute values of charge transfer, HOMO, LUMO, and $E_g$ are slightly lower than those of B3LYP. However, as in the B3LYP/6-31G(d), the B3PW91 method shows that the $E_g$ of functionalized SWNTs is significantly increased upon adsorption. This emphasizes that these nanotubes are highly sensitive to HCl. The change in the $E_g$ will be reliable, assuming cancellation of errors. Although the P3PW91 predicts the $E_{ad}$ values less negative than B3LYP, the order of $E_{ad}$ follows that of the B3LYP and the **C** complex has the least negative value.

In order to investigate the effect of HF percentage of density functional on the adsorption energies and electronic properties, the configuration **C** and its complex with HCl were selected and all calculations were repeated with four Minnesota functionals.[49-51] The functionals M06-L, M06, M06-2X, and M06-HF show 0, 27, 54, and 100% HF exchange, respectively. The adsorption energies (Table 4) become slightly more negative by increasing HF% exchange. This is due to the self-interaction errors of approximate density functionals.[42] The self-interaction error of a functional is decreased by increasing HF% exchange.[52] Table 4 shows that the HOMO, LUMO, and $E_g$ of the systems significantly vary by altering the density functional. On increasing the percentage of HF exchange, the LUMO and HOMO are stabilized and destabilized, respectively, hence increasing the $E_g$. Although absolute values of the LUMO, HOMO, and $E_g$ depend on the density functional, all of these demonstrate that the $E_g$ of **C** is sensitive toward HCl.

## Conclusions

We have investigated the sensing mechanism of a series of SWNT materials based on the electronic properties and work function changes toward HCl, and compared the results with the experimental reports. We have shown that the basic sites in the SWNTs play an important role in the detection of HCl. The HCl adsorption strongly influences the electronic properties of the functionalized SWNT by modulating the concentration of electrons in the valence or conduction levels. By exposing three functionalized SWNTs to HCl, we have shown that protonation of the basic group induces electron transfer from the semiconducting SWNTs thereby altering the HOMO and LUMO levels and significantly changing the electronic properties and work function.

## References


1 Peyghan A A, Baei M T, Hashemian S & Moghimi M, *Chinese Chem Lett*, 23 (2012) 1275.
2 Goodarzi Z, Maghrebi M, Zavareh A F, Mokhtari-Hosseini Z B, Ebrahimi-hoseinzadeh B, Zarmi A H & Barshan-tashnizi M, *J Nanostruct Chem*, 5 (2015) 237.
3 Samadizadeh M, Peyghan A A & Rastegar S F, *Chinese Chem Lett*, 26 (2015) 1042.
4 Mahdavian L, *J Nanostruct Chem,* 3 (2012) 1.
5 Baei M T, Peyghan A A & Z Bagheri, *Chinese Chem Lett*, 23 (2012) 965.
6 Beheshtian J, Peyghan A A & Noei M, *Sensors Actuators B: Chem,* 181 (2013) 829.
7 Najafi F, *J Nanostruct Chem,* 3 (2013) 1.
8 Peyghan A A, Noei M & Yourdkhani S, *Superlattices Microstruct,* 59 (2013) 115.
9 Noei M, Ebrahimikia M, Saghapour Y, Khodaverdi M, Salari A A & Ahmadaghaei N, *J Nanostruct Chem,* 5 (2013) 213.
10 1Beheshtian J, Ahmadi Peyghan A & Bagheri Z, *Struct Chem,* 24 (2013) 165.
11 Saha M & Das S, *J Nanostruct Chem,* 4 (2014) 1.
12 Feng X, Irle S, Witek H, Morokuma K, Vidic R & Borguet E, *J Am Chem Soc*, 127 (2005) 10533.
13 Soltani A, Ahmadi Peyghan A & Bagheri Z, *Physica E*, 48 (2013) 176.
14 Peyghan A A & Noei M, *Comput Mater Sci,* 82 (2014) 197.
15 Peyghan A A, Rastegar S F & Hadipour N L, *Phys Lett A*, 378 (2014) 2184.
16 Baei M T, Peyghan A A, Bagheri Z & Tabar M B, *Phys Lett A*, 377 (2012) 107.
17 Zare K, Gupta V K, Moradi O, Makhlouf A S H, Sillanpää M, Nadagouda M, Sadegh H, Shahryari-ghoshekandi R, Pal A, Wang Z, Tyagi I & Kazemi M, *J Nanostruct Chem,* 5 (2015) 227.
18 Beheshtian J, Peyghan A A & Bagheri Z, *Sensors Actuators B: Chem*, 171-172 (2012) 846.
19 Parlayici S, Eskizeybek V, Avcı A & Pehlivan E, *J Nanostruct Chem,* 5 (2015) 255.
20 Ahmadi Peyghan A, Hadipour N L & Bagheri Z, *J Phys Chem C*, 117 (2013) 2427.
21 Ghaffari A, Tehrani M S, Husain S W, Anbia M & Azar P A, *J Nanostruct Chem,* 4 (2014) 1.
22 Beheshtian J, Peyghan A A & Bagheri Z, *J Mol Model*, 19 (2012) 391.
23 Bekyarova E, Davis M, Burch T, Itkis M E, Zhao B, Sunshine S & Haddon R C, *J Phys Chem B*, 108 (2004) 19717.
24 Muthukumar P & John S A, *Sensors Actuators B: Chem*, 159 (2011) 238.
25 Matsuguchi M, Kadowaki Y, Noda K & Naganawa R, *Sensors Actuators B: Chem*, 120 (2007) 462.
26 Bekyarova E, Kalinina I, Sun X, Shastry T, Worsley K, Chi X, Itkis M E & Haddon R C, *Adv Mater*, 22 (2010) 848.
27 Grimme S, Antony J, Ehrlich S & Krieg H, *J Chem Phys,* 132 (2010) 154104.
28 Gordon M & Schmidt M, *Theory and Applications of Computational Chemistry: The First Forty Years,* (Elsevier, Amsterdam) 2005, p 1167.
29 Su N,Guo Q & Wu S, *Indian J Chem,* 47A (2008) 1473.
30 Ahmadi A, Beheshtian J & Kamfiroozi M, *J Mol Model*, 18 (2012) 1729.
31 Beheshtian J, Peyghan A A & Bagheri Z, Appl Surf S*ci*, 259 (2012) 631.
32 Zare K & Shadmani N, *J Nanostruct Chem,* 3 (2013) 1.
33 Beheshtian J, Peyghan A A & Bagheri Z, *Monatsh Chem,* 143 (2012) 1623.
34 Dinadayalane T C, Murray J S, Concha M C, Politzer P & Leszczynski J, *J Chem Theor Comput*, 6 (2010) 1351.
35 Nagarajan V, Chandiramouli R, Sriram S & Gopinath P, *J Nanostruct Chem,* 4 (2014) 1.
36 Tapas M, Shrabanti B & Sumanta B, *Indian J Chem*, 49A (2010) 1461.
37 Tomić S, Montanari B & Harrison N M, *Physica E*, 40 (2008) 2125.
38 Ahmadi A, Beheshtian J & Hadipour N L, *Struct Chem,* 22 (2011) 183.
39 Beheshtian J, Peyghan A A & Bagheri Z, *Comput Theor Chem*, 992 (2012) 164.
40 Ahmadi A, Hadipour N L, Kamfiroozi M & Bagheri Z, *Sensors Actuators B: Chem*, 161 (2012) 1025.
41 Rastegar S F, Peyghan A A & Hadipour N L, *Appl Surf Sci,* 265 (2012) 412.
42 Beheshtian J, Baei M T, Bagheri Z & Peyghan A A, *Microelectron J,* 43 (2012) 452.
43 Eisele I & Burgmair M, *Proc Conf*, *Optoelectronic and Microelectronic Materials and Devices, 2000. COMMAD 2000.* p 285.
44 Ueno N, *Physics of Organic Semiconductors*, (Wiley–VCH Verlag GmbH & Co KGAA) 2012, p 70.
45 Shiraishi M & Ata M, *Carbon*, 39 (2001) 1913.
46 Suzuki S, Watanabe Y, Homma Y, Fukuba S-y, Heun S & Locatelli A, *Appl Phys Lett*, 85 (2004) 127.
47 Dewar M, Zoebisch E G, Healy E F & Stewart J, *J Am Chem Soc*, 107 (1985) 3902.
48 Peyghan A A, Hadipour N & Bagheri Z, *J Phys Chem C*, 117 (2013) 2427.
49 Zhao Y & Truhlar D G, *J Chem Phys,* 125 (2006) 194101.
50 Zhao Y & Truhlar D G, *Theor Chem Acc*, 120 (2006) 215.
51 Zhao Y & Truhlar D G, *J Phys Chem A,* 110 (2006) 13126.
52 Cohen A, Mori-Sánchez P & Yang W, *Science,* 321 (2008) 792.